Optical Transmission through Periodically Nano-structured Metal Films

L. Martín-Moreno[1] and F. J. García-Vidal[2]

[1] Departamento de Física de la Materia Condensada
ICMA-CSIC, Universidad de Zaragoza, 50009 Zaragoza, Spain
[2] Departamento de Física Teórica de la Materia Condensada
Universidad Autónoma de Madrid, 28049 Madrid, Spain

Abstract. We present a review of some of the recent developments on the use of surface plasmons for subwavelength optics. As example of how surface plasmons are helping us to play new tricks with light, we focus on the optical transmission through *shape periodically* nano-structured metal films.

1 Introduction

In the last few years there has been a renewed interest in the optical properties of metallic structures. This interest is driven by the desire to reduce the dimensions of optical devices, which is becoming possible due to technological advances in the micro- and nano- patterning of metals.

The dielectric optical response of a metal is mainly governed by its free electron plasma. Below its plasma frequency, the real part of the dielectric constant (ϵ_M) of a metal is negative, so the wavevector of light propagating inside a metal has an imaginary component and the metal behaves as a photonic insulator. A negative ϵ_M has another important consequence: a metal surface may support localized electromagnetic (EM) resonances, called surface plasmons (SPs) [1]. These resonances propagate along the surface of a metal, and can be tailored to concentrate and guide light in very small volumes. For optical frequencies, SPs appearing in good metals (like silver) may propagate distances of the order of $10 - 100\,\mu$m before being absorbed, going up to 1 mm in the near infrared. Therefore, if we are interested in highly integrated planar optical devices smaller than these typical propagation distances, the inherent absorption present in conductive systems could be not a too serious drawback, and SPs could be considered as a promising route to sub-wavelength optics [2].

In the first part of this paper we overview some of the recent developments on the use of SPs for subwavelength optics. As example of these new capabilities, in the second part of the paper we focus on the optical transmission through *shape periodically* nano-structured metal films.

B. Kramer (Ed.): Adv. in Solid State Phys. **44**, 69–80 (2004)

2 SPs as a Route to Sub-wavelength Optics

The dispersion relation of a SP propagating in a metal-vacuum interface is given by the following equation

$$k(\omega) = \frac{w}{c}\sqrt{\frac{\epsilon_M(\omega)}{1+\epsilon_M(\omega)}} \tag{1}$$

where ω is the frequency, c is the speed of light and $\epsilon_M(\omega)$, the frequency-dependent dielectric constant of the metal.

As its dispersion curve lies outside the light-cone, a SP on a metal surface can not be excited by an incident plane wave. This is the main problem when dealing with these type of surface EM resonances: the coupling of light into SPs and the reversed process, coupling SPs to light. There are three main different strategies to overcome this difficulty.

The most common technique to excite SPs consists in evaporating a thin metal film onto an optically dense substrate. Illuminating through the substrate at an angle of incidence slightly larger than the critical angle allows the wave vector of the incident light to match that of the SP. This technique, known as attenuated total reflection (ATR) [3], has been used recently to analyze the propagation of SPs on thin metal stripes [4]. These metal stripes could be used in optoelectronic devices as a common channel to propagation of both electrical current and light via SPs.

The second approach consists in launching SPs by focusing a laser beam onto a topological defect [5]. Combining this technique with fluorescence imaging, it has been possible to test the first realizations of a SP-based Bragg mirror and a SP-based beam-splitter [6]. These promising results could open the possibility of using SPs in order to create devices able to do sub-wavelength optics in two dimensions.

The third way for coupling light into SPs is by creating a periodic modulation of the metal surface. This modulation provokes the folding of the SP bands inside the first Brillouin zone, i.e., inside the light cone. Already in 1902, Wood [7] reported anomalous behaviour in the diffraction of light by metallic gratings that we now know were due to the excitation of SPs. Periodicity can also lead to the opening of a full photonic band gap (PBG) in the SP spectrum, in a way very much similar to the opening of a photonic band gap in photonic crystals. By analyzing the reflectance spectrum of an hexagonal array of photoresist dots on a glass substrate coated with a thin film of silver, Kitson *et al.* [8] were able to report the appearance of a SP-PBG between 1.91 and 2.0eV, within the visible range of EM spectrum. The existence of a band gap in which light propagation is forbidden can lead to many optical applications. Among others, it is possible to guide light in two-dimensions by just creating some line defects into the periodic array: light with the appropriate energy inside the gap can not couple to bulk crystal EM modes and its propagation is confined inside the line defect. Experimental realization of

these ideas has been recently reported [9], rendering the prospect of photonic circuits based on SPs.

3 Optical Transmission Through Nano-structured Metals

In 1998, Ebbesen et al. [10] found experimentally that the transmission of light through subwavelength hole arrays made in a metal film may be, for some particular resonant wavelengths, orders of magnitude larger than expected if the holes were acting *shape independently*. Standard aperture theory stated that, for a single hole, the transmittance (T), is roughly $T \sim a^2\,(a/\lambda)^4$ (a being the hole radius) [11], *shape i.e.* due to the wave character of the light the normalized-to-area transmittance through a hole is very small whenever $a << \lambda$. Furthermore, that theory was done for the case of a metal film with infinitesimal thickness; for the realistic case of finite metal thickness the transmittance should be even smaller as, in the subwavelength limit, all EM modes inside the waveguide are evanescent. It is worth pointing out that, before Ebbesen's experiment, hole arrays had been extensively studied, due mainly to their properties as selective filters. For this, the high-pass filtering properties are provided by the hole EM cutoff, while the low-pass filter is due to the redistribution of energy caused by the periodic array when a new diffraction order becomes propagating. More precisely, denoting the hole cut-off wavelength by λ_c, and the lattice parameter by d, hole arrays were known to act as band-pass filters for $d < \lambda < \lambda_c$. This property has been studied in several frequency regimes. as microwave [12], far infrared [13], mid infrared [14] and infrared [15]. However, the extraordinary optical transmission (EOT) discovered by Ebbesen et al. presented two main differences with previous works. First, experiments were performed in the optical regime, and second, the geometrical parameters defining the structure were such that $\lambda_c < d < \lambda$; this parameter range had not, up to our knowledge, been studied before, perhaps because nothing remarkable was expected for wavelengths beyond cut-off. Although already the first experiments [10] showed that EOT was related to the excitation of SPs, the transmission mechanism was unclear. The initial theoretical efforts concentrated on the simpler system of a periodic array of 1D apertures (slits), with realistic calculations for the 2D Ebbesen's geometry appearing shortly afterwards. Here we review the basics of the enhanced transmission phenomena for both the 1D- and 2D-array of apertures in an opaque metal film.

3.1 1D Slit Array

Consider the transmission grating (TG) depicted in Fig. 1 (find there also the definition for the different geometrical parameters defining the array and the choice of axis).

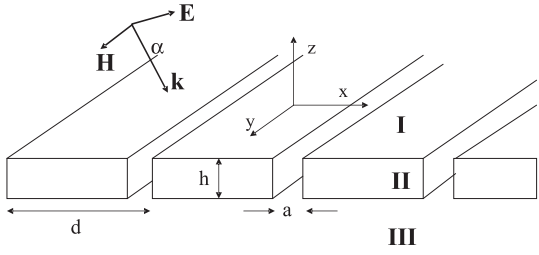

Fig. 1. Scheme of a 1D array of slits in a metal film. Regions I and III are filled by a dielectric materials, that here we take to be air in both cases

This system is reminiscent of reflection gratings, in which case region III in Fig. 1 is filled with metal. Reflection gratings have been extensively studied in the past. As commented in the introduction, Wood [7] found remarkable absorption anomalies in the reflectance spectra of smooth metallic gratings illuminated by p-polarized light (E-field perpendicular to the grating axis). Fano [16] associated these anomalies to the excitation of SPs. Later on, Hessel and Oliner found [17] another type of absorption anomaly, appearing in deep gratings, associated to the formation of standing waves inside the grooves. The small volume of these modes results in strong EM field enhancement, so these systems are excellent substrates for surface-enhanced Raman studies [20].

Apart from some theoretical works [18,19], TGs had not received so much attention, but after Ebbesen's experiment they have been thoroughly studied. TGs have proved interesting in their own right, and some of the basics of the enhanced transmission phenomena are already present in these systems. However it must be kept in mind that in a slit waveguide there is always a propagating mode inside the waveguide, no matter how narrow it is, while a hole waveguide present a cutoff frequency and all modes are evanescent for hole diameters smaller than (roughly) half a wavelength. Therefore, wave propagation is radically different for slits and holes.

3.1.1 Theoretical Formalism

Let us concentrate on the optical transmission properties of arrays of subwavelength slits, for p-polarized light. For s-polarization (E-field along the slit axis) the transmission does not present such a rich resonant behavior, and will not be discussed here. There are different theoretical frameworks that give virtually exact results for the transmittance of such a simple structure. However, the physical mechanisms responsible for the transmittance spectra are best captured by a simplified quasi-analytical model, where fields are represented in different regions by a modal expansion [21]. We have previously demonstrated [22] the accuracy of this theoretical framework in comparison with, for example, transfer matrix methods. Two main approximations are considered within our modal expansion:

- only the fundamental eigenmode in the modal expansion of the EM fields inside each slit is considered, which is justified because in the subwavelength regime the fundamental mode is the only propagating one, and dominates the transmittance
- surface impedance boundary conditions (SIBC) [23] are imposed on the metal dielectric interfaces. The approximation of SIBC is applicable when the skin depth in the metal (of the order of $20\,nm$, for good metals in the optical regime) is much smaller than all other length scales in the system. Strictly, this is not the case, as we are going to consider slit widths of a few tens of nanometers. However, as the propagation constant of the fundamental mode of the slit does not depend on slit width, it turns out that the SIBC is a good approximation for this kind of systems even in the optical regime. Moreover, given that in the considered structures the "horizontal" metal-dielectric interfaces are much larger that the "vertical" ones, we further simplify the model (just for computational convenience) by assuming that the vertical walls of the slits are perfect metal surfaces.

For p-polarization, the modal expansion for the magnetic field is

$$
\begin{aligned}
H_y(x,z) &= \Psi_0^+(x,z) + \sum_n r_n \Psi_n^-(x,z), \quad \text{for } z \text{ in region I} \\
H_y(x,z) &= \sum_m \left\{ A_m \Phi_m^+(x,z) + B_m \Phi_m^-(x,z) \right\}, \quad \text{for } z \text{ in region II} \\
H_y(x,z) &= \sum_n t_n \Psi_n^+(x,z), \quad \text{for } z \text{ in region III.}
\end{aligned} \tag{2}
$$

where, for an incident wave impinging at angle α with the normal, $k = \omega/c$, $k_{xn} = k\cos(\alpha) + (2\pi/d)n$, $k_{zn} = \sqrt{k^2 - k_{xn}^2}$, $\Phi_m^{\pm}(x,z) = \exp(\pm \imath k z)/\sqrt{d}$ if $x \epsilon\, [md - a/2, md + a/2]$ and zero otherwise, and $\Psi_n^{\pm}(x,z) = \exp(\imath k_{xn} x \pm \imath k_{zn} z)/\sqrt{d}$. In Eq. 2, all summations go from $-\infty$ to $+\infty$. The electric field components E_x and E_z, can be readily calculated via the Maxwell equation $\nabla \times \boldsymbol{E} = ik\boldsymbol{H}$.

Calculating the transmission and reflection coefficients t_n and r_n into the different diffraction orders, and the slit amplitudes A_m and B_m is a simple exercise of matching fields at both I-II and II-III interfaces. However, it is convenient to extract the scattering coefficients in the three-region system from the scattering coefficients of two independent two-region systems: the I-II and the II-III systems, in which all regions are taken as semi-infinite (even region II). Let us concentrate on the zero-order transmission amplitude, t_0; expressions for all other scattering amplitudes can be calculated trivially in a similar manner. We define (see Fig. 2) the scattering coefficients in the two-region systems as follows: in the I-II system, an incident plane wave coming from region I reflects, when reaching I-II interface, with probability amplitude ρ^{11} or transmits through the interface with amplitude τ^{12}. When approaching the II-I interface coming from region II, the slit fundamental eigenmode

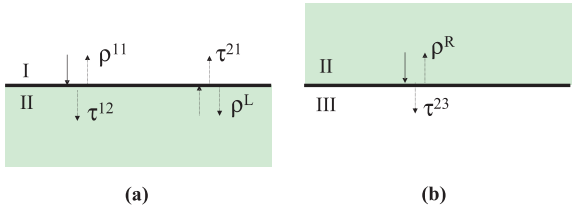

Fig. 2. Definitions of the different scattering coefficients of the two different two-region systems appearing in transmission gratings

either reflects with amplitude ρ^{L}, or transmits to region I with amplitude τ^{21}. Actually, ρ^{11} and τ^{21} would be matrices, given that the final state could be any of the diffraction orders. In the II-III system, the propagating mode coming from region II bounces back at the II-III interface with amplitude ρ^{R} or transmits to region III with amplitude τ^{23}.

Knowing all these coefficients, the scattering coefficients for the real three-region system can be easily calculated summing up all multiple scattering processes, the only additional ingredient needed is the phase accumulated by the EM field when propagating inside the waveguide, $\phi_P = \exp(\imath\theta_P)$, with $\theta_P = kh$. The final result is

$$t_0 \;=\; \frac{\tau^{12}\,\phi_P\,\tau^{23}}{1\;-\;\rho^{\mathrm{L}}\,\rho^{\mathrm{R}}\,\phi_P^2} \tag{3}$$

The expressions for the different two-region coefficients can be found in [22]. Let us just recall that

$$\rho^{\mathrm{L}} \;=\; \rho^{\mathrm{R}} \;=\; -\,\frac{1\;-\;(1+Z_s)\,f}{1\;+\;(1-Z_s)\,f} \tag{4}$$

where $Z_s = [\epsilon(\omega)]^{-1/2}$ is the metal surface impedance and

$$f \;=\; \sum_{n=-\infty}^{n=+\infty} \frac{[\mathrm{sinc}(k_{xn}a/2)]^2}{k_{zn}/k + Z_s} \tag{5}$$

where $\mathrm{sinc}(x) = \sin(x)/x$, and f is a quantity that plays a central role in all scattering coefficients. A crucial point, which strongly influences the transmission (and reflection) properties is that f is singular whenever any of the diffraction orders satisfy $k_{zn} = -kZ_s$, which is the condition for existence of a SP on a *shape flat* metal surface (within the SIBC approximation).

3.1.2 Results

Let us consider a slit array made in silver film [24] with $d = 1.75\,\mu\mathrm{m}$, $a = 0.30\,\mu\mathrm{m}$ and $W = 0.4\,\mu\mathrm{m}$, which are typical experimental parameters [25], illuminated by an normal-incident p-polarized EM field. We concentrate in

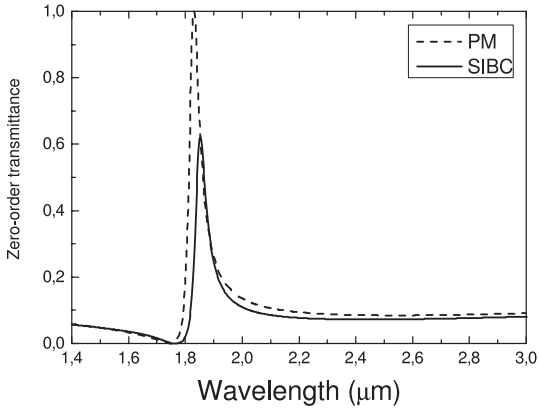

Fig. 3. Comparison between $T(\lambda)$ calculated with our simplified modal expansion for surface impedance (full curve) and perfect metal (dashed curve) boundary conditions. The geometrical parameters are: $d = 1.75\,\mu\text{m}$, $a = 0.3\,\mu\text{m}$ and $W = 0.4\,\mu\text{m}$ for normal-incident p-polarized light

the spectral region $\lambda > d$, where only the zero-order transmission coefficient t_0 contributes to the total current.

Figure 3 renders the comparison between the transmittance spectra calculated with the simplified modal expansion previously described, and the calculation in which SIBC are substituted by perfect metal (PM) boundary conditions.

As Fig. 3 shows, the transmittance spectrum presents a peak, where light is almost 100% transmitted for the PM case. This is reduced by around 40% when the absorption in the metal is included.

In order to gain physical insight into the origin of this transmission peak, it is convenient to rewrite $\rho^{\mathrm{L}} = R\,\exp(\imath\theta_S)$. Then, defining $\theta_T = 2\,(\theta_P + \theta_S)$, t_0 can be written as

$$t_0 = \frac{\tau^{12}\,\phi_P\,\tau^{23}}{1 - R^2\,\exp(\imath\theta_T)} \tag{6}$$

For narrow slits, due to the large impedance mismatch, $R \approx 1$ (as the slit waveguide mode is propagating, current conservation forces R to range from 0 to 1), so the transmittance is dominated by the total phase θ_T. Therefore, the system behaves as a Fabry-Perot interferometer: whenever θ_T in an integer times 2π, all partial waves in the multiple scattering series interfere constructively in the forward direction, leading to a maximum in $T(\lambda)$. However, as a difference with a standard Fabry-Perot interferometer, added to the wavelength dependence of the optical-path phase θ_P, the scattering phase (θ_S) varies strongly close to the SPs spectral locations. This is illustrated in Fig. 4, showing θ_T and T as a function of wavelength, for different metal thicknesses.

Figure 4 shows a series of transmittance peaks, reaching 100% transmission if absorption is neglected. Notice that the slit only occupies a small fraction of the device unit cell, so the structured metal surface is acting as a funnel, collecting all light impinging on the surface into a very narrow

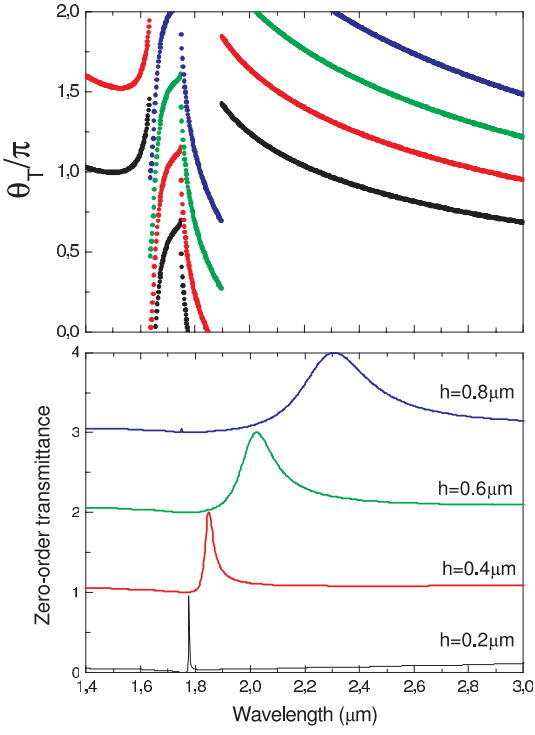

Fig. 4. Total phase θ_T (panel (a)) and zero-order transmittance (panel (b)) as a function of λ, for a normal-incident p-polarized plane-wave impinging on a slit array with $d = 1.75\,\mu$m, $a = 0.3\,\mu$m for different thicknesses: $W = 0.2, 0.4, 0.6$ and $0.8\,\mu$m. Each transmittance curve has been shifted by $+1$ with respect to the previous one for better visualization

aperture. These resonances present large differences in peak linewidths (and, correspondingly, the sensitivity to absorption). It can be shown that the resonance linewidth is inversely proportional to the derivative of θ_T with respect to λ, which is large (due to the behavior of θ_S whenever there is a surface resonance in the system). Also the EM field distribution changes from being mostly the one corresponding to two coupled SPs, to having a cavity mode character (reminiscent of the open-organ pipe modes), depending on whether the peak spectral position is close to the $k_{zn} = kZ_s$ condition or away from it, respectively [22].

3.2 2D Hole Array

As previously stated, the studies of slit arrays are of limited value for understanding the transmission through subwavelength hole arrays, given that a subwavelength hole does not support a propagating TEM mode, while a subwavelength slit does. Computation of the transmittance for hole arrays is much more computationally demanding than for slit arrays, due to the lower symmetry in the former system. Popov et al. [26] presented a calculation based on a modal expansion taking into account the spectral dependence of the dielectric constant in the metal, $\epsilon_M(\omega)$. Their calculations showed transmission peaks, which were associated to an EM mode propagating along the

holes, that appeared in the hole array when a realistic $\epsilon_M(\omega)$ was taken into account, and was not present when the metal was treated as perfectly conducting. On the contrary, a calculation performed with a modal expansion plus the approximations previously described for the slit array calculation, reported EOT, *shape even in the metal were perfectly conducting* [27]. Here we adhere to this last view, and present what we believe are the basics of the EOT phenomena in 2D hole arrays, by studying for a highly simplified model. This model treats the metal as a perfect conductor, showing that EOT is possible even when there is no propagating mode inside the holes.

3.2.1 Minimal Model

The calculation for the transmittance through an square array of square holes, within the approximations described in the subsection 3.1.1, was presented in [27]. In this case, all diffraction orders (resulting from a change in the incident parallel momentum by a reciprocal lattice vector), as well as both polarizations must, in principle, be taken into account. However, a minimal model, which considers just the incoming wave plus two diffraction orders (for a normal-incident linearly-polarized incoming wave, with the E-field pointing along the x-direction, we consider the p-polarized diffraction order with $k_x = 0, \pm 1$ times $2\pi/d$) provides an excellent approximation to the transmittance spectra. In this paper, we also treat the metal as perfectly conducting ($Z_s = 0$). This approximation further simplifies the calculation; considering absorption in the metal would reduce the transmission peaks [27] but would not alter the physical picture [29]. Figure 5 shows the comparison between the $T(\lambda)$, for a square array of square holes [30] calculated with this minimal model.

Clearly, the minimal model captures the physics of the EOT, with the advantage that it can be analytically worked out. It this case, the multiple scattering series (3) gives

$$t_{00} = \frac{\tau^{12}\, e^{-|q|W} \tau^{23}}{1 - \rho^2\, e^{-2|q|W}} \tag{7}$$

where, denoting $q = \sqrt{k^2 - (\pi/a)^2}$, $k_{z1} = \sqrt{k^2 - k_{x1}^2}$, $S_0 = 2\sqrt{2}a/(\pi d)$, $S_1 = S_0\,\mathrm{sinc}\,[k_{x1}d/2]$, $G_1 = S_0^2 + 2S_1^2 k/k_{z1}$ and $G_2 = q/k$, it is found that $\tau^{12} = 2S_0/(G_2 + G_1)$, $\tau^{23} = 2G_2/(G_2 + G_1)$, and $\rho = (G_2 - G_1)/(G_2 + G_1)$.

The appearance of EOT is related to resonant denominators in Eq. (7), which are possible because, for evanescent modes, current conservation only forces $\mathrm{Im}(\rho) > 0$, but says noting about the modulus of ρ. This point is illustrated in Fig. 5, showing both real and imaginary parts of $\rho(\lambda)$. As ρ is a causal function, its real and imaginary part must satisfy Kramers-Kronig relations; furthermore, the peak in $\mathrm{Im}(\rho)$ signals the presence of a localized surface EM mode in the system (the peak in $|\rho|$ in Fig. 5 is due to a peak in $\mathrm{Im}(\rho)$). The finite spectral width of this peak is inversely proportional to

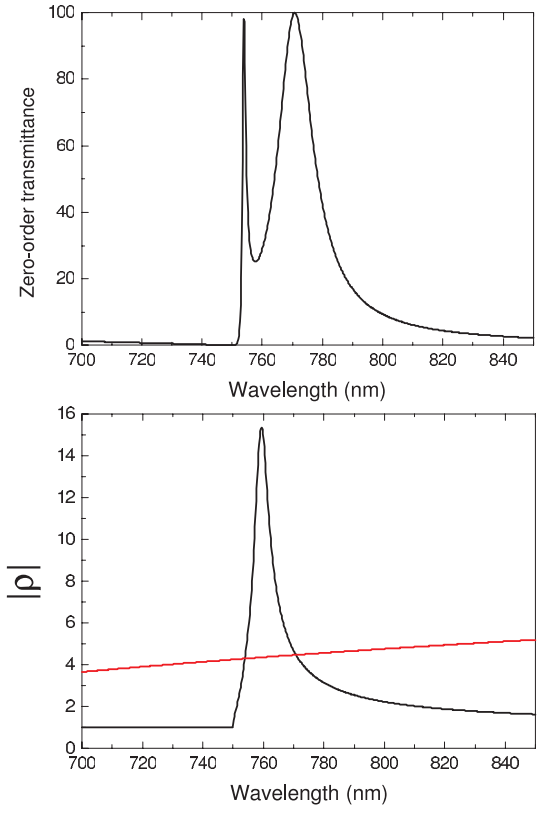

Fig. 5. Upper panel: $T(\lambda)$, for a square array of holes in a perfect metal, calculated within the minimal model, for normal-incident p-polarized light. Lower panel: $|\rho(\lambda)|$ (black curve) and $e^{|q|W}$. When this two magnitudes are equal, there is a peak in $T(\lambda)$. We consider d=750 nm, W=200 nm and square holes with side length a=284 nm (in order to mimic circular holes with a diameter of 320 nm)

the time that the EM takes to leave the system due to radiation losses ($t_{\rm rad}$), so more precisely speaking, what the system develops is a leaky surface EM mode. There are two such modes (one for each metal-dielectric interface), which are coupled through the evanescent fields inside the holes. This results in symmetric and antisymmetric combinations, in much the same way electronic states of isolated atoms combine to form molecular levels [27]. The case of transmission through holes in a metal film resting on a dielectric substrate was described in [28] and, in this picture, it would correspond to the formation of surface plasmon "molecular levels" (SPML) from non-equal surface plasmon "atoms". This "surface plasmon molecular states" are coupled to radiation modes, and EOT occurs via them. In this sense it can be stated that EOT is the physics of two localized levels coupled to a continuum. Additional insight can be gained if we calculate the SPML spectral position neglecting the coupling to the radiative modes. In this case, from the frequency difference between the position of this modes is related to the time the photon has to stay in the system in order to "see" the resonant levels, $t_{\rm res}$. Notice that $t_{\rm res}$ depends on the coupling between SPs, i.e., on metal thickness, while $t_{\rm rad}$ does not, as it is a characteristic of a single surface. Different regimes

of tunnelling (sequential for $t_{\mathrm{rad}} < t_{\mathrm{res}}$ and resonant) in the opposite case were predicted [27] (see also Ref. [31] for a description of similar physics in resonant tunnelling in quantum mechanics) and measured subsequently [32].

3.3 Single Apertures Flanked by Corrugations

We would like to end with a short note on non-periodic systems. As was discussed, surface EM waves were at the heart of the EOT phenomena. However, it was reasonable to think that perfect periodicity was not strictly necessary for the existence of surface waves, This opens the possibility of using SPs in order to obtain EOT through a *shape single aperture*, effect that has now been studied both experimentally [33] and theoretically [34], if the metal surface is corrugated in the side the light is impinging on. Moreover, it has been found that very strong directional emission is possible through single apertures if the corrugation is on the exit side [35,36,37]. Recently, light demultiplexing [38] and focusing effects [39] have been reported in single apertures in corrugated metals. It might well be that, although based on guiding ideas found when studying periodic systems, many surprises and applications are still to be found in finite non-periodic systems.

Acknowledgements

We would like to acknowledge financial support by the Spanish MCyT through contracts MAT2002-01534 and MAT2002-00139, and fruitful discussions and collaborations with J. Bravo-Abad, T.W. Ebbesen, H.J. Lezec, J.A. Porto, T. Thio and J.B. Pendry.

References

1. R.H. Ritchie, Phys. Rev. **106**, 874 (1957). 69
2. W.L. Barnes, A. Dereux, and T.W. Ebbesen, Nature **424**, 824 (2003). 69
3. E. Kretschmann and H. Raether, Z. Naturforsch. A **23**, 2135-2136 (1968); A. Otto, Z. Phys. **216**, 398 (1968). 70
4. J.C. Weeber *et al.*, Phys. Rev. B **64**, 0455411 (2001). 70
5. B. Hecht, H. Bielefeldt, L. Novotny, Y. Inouye, and D.W. Pohl, Phys. Rev. Lett. **77**, 1889 (1996). 70
6. H. Ditlbacher, J.R. Krenn, G. Schider, A.Leitner, and F.R. Aussenegg, Appl. Phys. Lett. **81**, 1762 (2002). 70
7. R.W. Wood, Phil. Mag. **4**, 396 (1902). 70, 72
8. S.C. Kitson, W.L. Barnes, and J.R. Sambles, Phys. Rev. Lett. **77**, 2670 (1996). 70
9. S.I. Bozhevolnyi, J. Erland, K. Leosson, P.M.W. Skovgaard, and J.M. Hvam, Phys. Rev. Lett. **86**, 3008 (2001); S.I. Bozhevolnyi, V.S. Volkov, K. Leosson, and A. Boltasseva, Appl. Phys. Lett. **79**, 1076 (2001). 71
10. T.W. Ebbesen, H.J. Lezec, H.F. Ghaemi, T. Thio, and P.A. Wolff, Nature **391**, 667 (1998). 71

11. H. A. Bethe, Phys. Rev. **66**, 163 (1944). 71
12. F. Keilmann, Int. Journ. Infrared and Millimeter Waves **2**, 259 (1981). 71
13. A. Mitsuishi, Y. Otsuka, S. Fujita and H. Yoshinaga, Jap. J. Appl. Phys., **2**, 574 (1963). 71
14. R. Ulrich, Infrared Phys., **7**, 27 (1967). 71
15. C.M. Rhoads, E.K. Damon, and B.A. Munk, Appl. Opt. **21**, 2814 (1982). 71
16. U. Fano, J. Opt. Soc. Am. **31**, 213 (1941). 72
17. A. Hessel and A.A. Oliner, Appl. Opt. **4**, 1275 (1965). 72
18. H. Lochbihler, Phys. Rev. B **50**, 4795 (1994). 72
19. J.J. Kuta *et al.*, J. Opt. Soc. Am. A **12**, 1118 (1995). 72
20. F.J. Garcia-Vidal and J.B. Pendry, Phys. Rev. Lett. **77**, 1163 (1996). 72
21. P. Sheng, R.S. Stepleman, and P.N. Sanda, Phys. Rev. B **26**, 2907 (1982). 72
22. F.J. Garcia-Vidal and L. Martin-Moreno, Phys. Rev. B **66**, 155412 (2002). 72, 74, 76
23. L.D.Landau, E.M. Lifshitz and L.P. Pitaievskii, *Electrodynamics of Continuous Media*, Pergamon Press, second edition, (1994). 73
24. We take the dielectric constant for silver from: *Handbook of Optical Constants of Solids* , edited by E.D. Palik (Academic, Orlando, 1985). 74
25. A. Barbara, P. Quemerais, E. Bustarret, and T. Lopez-Rios, Phys. Rev. B **66**, 161403 (2002). 74
26. E. Popov, M. Nevière, S. Enoch, and R. Reinisch, Phys. Rev. B **62**, 16100 (2000). 76
27. L. Martin-Moreno, F.J. Garcia-Vidal, H.J. Lezec, K.M. Pellerin, T.Thio, J.B. Pendry, and T.W. Ebbesen, Phys. Rev. Lett. **86**, 1114 (2001). 77, 78, 79
28. A. Krishnan *et al.*, Opt. Comm. **200**, 1 (2001). 78
29. The effect of the field penetration inside the metal can be approximately taken into account by adding a skin depth to the hole lateral dimensions. 77
30. The choice of square holes is motivated by analitycal convenience. We have checked that an array of circular subwavelength holes present very similar transmittance spectra. 77
31. A. A. Abrikosov, Phys. Rev. B **66**, 212501 (2002). 79
32. A. Degiron, H. J. Lezec, W. L. Barnes, and T. W. Ebbesen, Appl. Phys. Lett. **81**, 4327 (2002). 79
33. T. Thio et al. Opt. Lett. **26**, 1972 (2001). 79
34. F. J. García-Vidal, H. J. Lezec, T. W. Ebbesen, and L. Martín-Moreno, Phys. Rev. Lett. **90**, 213901 (2003). 79
35. H. J. Lezec, A. Degiron, E. Deveaux, R.A. Linke, L.Martín-Moreno, F.J. García-Vidal and T.E. Ebbesen, Science **297**, 822 (2002). 79
36. A.P. Hibbins, J.R. Sambles and C.R. Lawrence, Appl. Phys. Lett. **81**, 4661 (2002). 79
37. L. Martín-Moreno, F. J. García-Vidal, H. J. Lezec, A. Degiron, and T. W. Ebbesen, Phys. Rev. Lett. **90**, 167401 (2003). 79
38. J. Bravo-Abad, F. J. García-Vidal and L. Martín-Moreno, Photonics and Nanostruct. **1**, 55 (2003). 79
39. F. J. García-Vidal, L. Martín-Moreno, H. J. Lezec and T. W. Ebbesen, Appl. Phys. Lett. **83**, 4500 (2003). 79